Journal of ELECTRONIC MATERIALS, Vol. 46, No. 10, 2017
DOI: 10.1007/s11664-017-5652-0

Modeling of Thermoelectric Generator Power Characteristics for Motorcycle-Type Engines

ALEXEY OSIPKOV,[1,2] ROMAN POSHEKHONOV,[1]
GEORGY ARUTYUNYAN,[1] ANDREY BASOV,[1] and ROMAN SAFONOV[1]

1.—Bauman Moscow State Technical University, 2-ya Baumanskaya St. 5, Moscow, Russia 105005.
2.—e-mail: alexosipkov@mail.ru

Thermoelectric generation in vehicles such as motorcycles, all-terrain vehicles, and snowmobiles opens the possibility of additional electrical energy generation by means of exhaust heat utilization. This is beneficial because replacing the mechanical generator used in such vehicles with a more powerful one in cases of electrical power deficiency is impossible. This paper proposes a calculation model for the thermoelectric generator (TEG) operational characteristics of the low-capacity internal combustion engines used in these vehicles. Two TEG structures are considered: (1) TEG with air cooling and (2) TEG with water cooling. Modeling consists of two calculation stages. In the first stage, the heat exchange coefficients of the hot and cold exchangers are determined using computational fluid dynamics. In the second stage, the TEG operational characteristics are modeled based on the nonlinear equations of the heat transfer and power balance. On the basis of the modeling results, the dependence of the TEG's major operating characteristics (such as the electrical power generated by the TEG and its efficiency and mass) on operating conditions or design parameters is determined. For example, the electrical power generated by a TEG for a Yamaha WR450F motorcycle engine with a volume of 0.449×10^{-3} m^3 was calculated to be as much as 100 W. Use of the TEG arrangements proposed is justified by the additional electrical power generation for small capacity vehicles, without the need for internal combustion engine redesign.

Key words: Thermoelectric generator, internal combustion engine, electrical power, efficiency, temperature problem, exhaust heat utilization, modeling

INTRODUCTION

Thermoelectric generation in vehicles such as motorcycles, all-terrain vehicles (ATVs), and snowmobiles opens the possibility of additional electrical energy generation by means of exhaust heat utilization. This is particularly relevant in the event of electrical power deficiency resulting from increased onboard power consumption. This paper proposes a calculation model for the thermoelectric generator (TEG) operational characteristics of the low-capacity internal combustion engines used in these vehicles. The prospects of TEG for vehicles are evident in recent research on TEG prototypes for motorcycles[1] and cars.[2–4]

For motorcycle-type engines, in most cases, the electromechanical generator is mounted coaxially on the crankshaft inside the motor case, which results in an absence of pulleys for accessory drives. Therefore, replacing a mechanical generator with a more powerful one in cases of electrical power deficiency is impossible. However, TEG installation in the exhaust line may be an effective solution for such electrical power deficiency.

(Received June 1, 2016; accepted June 12, 2017; published online June 26, 2017)

The calculation model proposed in this paper determines the TEG key performance characteristics (electrical power, efficiency, and mass) depending on the internal combustion engine (ICE) type and operating modes. Modeling the TEG operational characteristics in specific operating conditions requires consideration of multiphysical phenomena (such as thermal and electrical conductivity, convective heat exchange, fluid dynamics, and thermoelectric effects). Advanced computer-aided engineering program (CAE) packages enable multiphysical modeling of the TEG.[5] However, using them to optimize TEG construction is complicated. Parametric optimization requires multiple solutions, and topological optimization (when the number or mutual arrangement of the boundaries is changed) is complicated by the need for automatic determination of the boundary conditions. Thus, CAE packages are generally used to model the individual parts of the TEG[6] or the refinement and verification of numerical analysis models.[7]

In this paper, we combine an earlier nonlinear mathematical model of the TEG based on the nonlinear equations of heat transfer and power balance,[8] with the CAE model used to refine the heat exchange coefficients of the heat exchangers under specified operating conditions. The design under consideration is a prototype. For commercial introduction in the future, it is necessary to carry out parametric optimization and to ensure low contact resistance at the heat-conducting junctions. When using TEG in internal combustion diesel engines, it is necessary to solve the problem of soot deposition on the TEG inner surface as, over time, soot can significantly impair the heat transfer from the exhaust gases. For instance, Kajikawa[1] demonstrated that soot deposition can cause the heat flow from the TEG to be reduced by 25% in 200 h of operation. Sooting is much lower in gasoline engines; thus, the use of TEG in gasoline engines looks more promising.

Calculations were made for several TEG arrangements proposed for the Yamaha WR450F motorcycle-type internal combustion (IC) engine.

TEG Structural Arrangement

Two thermoelectric generator arrangements (air- and water-cooled) are considered (Fig. 1). The following sections of the TEG are indicated in Fig. 1: (1) hot heat exchanger, (2) thermoelectric battery, and (3) cold heat exchanger. The heat exchangers and the thermoelectric batteries are installed as sections lengthwise, in the direction of the hot air flow.

The ram air (in the air-cooled arrangement) is heated as it flows alongside the external fins of the cold heat exchanger. In contrast, the exhaust gases are cooled as they pass through the TEG. The heat exchangers of the TEG differ structurally in order to enable a uniform temperature drop at the section junctions.

Figure 2 presents the general schematic of a TEG, with the main temperatures and thermal flows shown. The TEG consists of i sections, each comprising cold and hot heat exchangers and a thermoelectric battery. A part of the power generated is used for forced cooling in the water-cooled TEG.

CHARACTERISTICS OF TEG MODELING

Modeling is performed in two stages. In the first stage, the heat-exchange coefficients of the hot and cold heat exchangers are determined via computational fluid dynamics (CFD). This includes modeling of the physical processes, such as the fluid dynamics of the air and exhaust flows with consideration for the geometry of the heat exchangers, and heat transfer in the structural metal components. In the second stage, the TEG operational characteristics are modeled based on the mathematical model developed in Ref. 8.

CFD Modeling

A CFD simulation of the physical processes was performed using the Flow Simulation software package to determine the heat transfer and thermal conductivity coefficients of the TEG. Favre averaged Navier–Stokes equations with the modified k–ε turbulence model were used to describe the flow of exhaust gases, whereas the steady-state flow of the homogenous exhaust gases was modeled with a finite volume method. The boundary conditions used in the simulation are given in Table I.

For the water-cooled TEG, only the exhaust gas flow inside the hot heat exchanger was simulated. For the air-cooled TEG, the external flow of the ambient air around the TEG was also modeled. In the preliminary assessment of the air-cooling efficiency, it was assumed that the TEG is placed in laminar air flow without any disturbances caused by other systems. The simulation enabled definition of the heat distribution in the various sections of the TEG and estimation of the heat transfer coefficients α_c (cold heat exchanger, air cooling only) and α_h (hot heat exchanger) (Fig. 3 and Table II).

Mathematical Simulation in MATLAB

Heat movement through each section of the TEG is treated as uniform heat movement through a set of parallel plates with varying areas and heights. Thermoelectric effect modeling is based on Marchenko's method.[9]

The calculation is performed successively for each TEG section. Those powers are summarized as follows: $Q_{hot} = \sum_i Q^i_{hot}$, $W_{teb} = \sum_i W^i_{teb}$, and the TEG efficiency is averaged $\eta_{teg} = \sum_i Q^i_{hot}(\sum_i W^i_{teb} - W_{Lost})^{-1}$. For calculation purposes, it is assumed that the electrical power losses over the TEG systems operation are zero for the air cooling

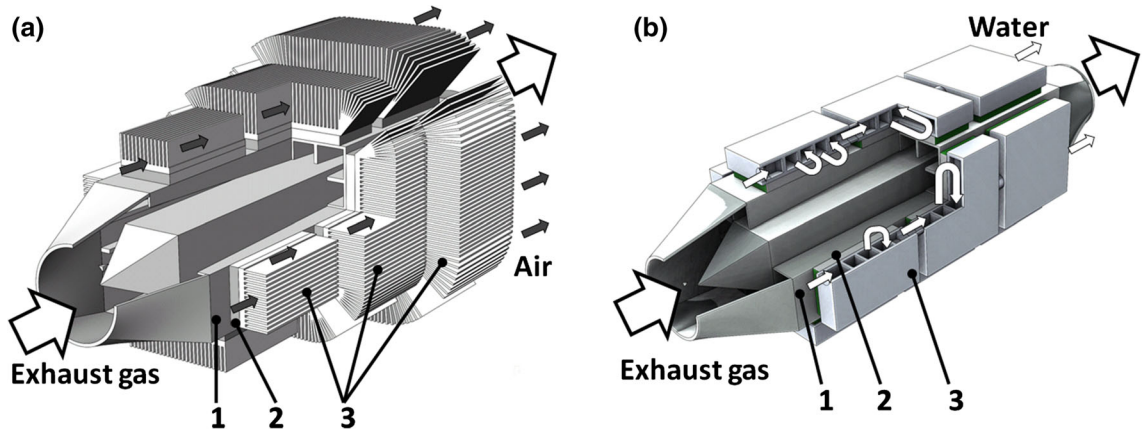

Fig. 1. TEG structures under consideration: (a) air cooled, (b) water cooled.

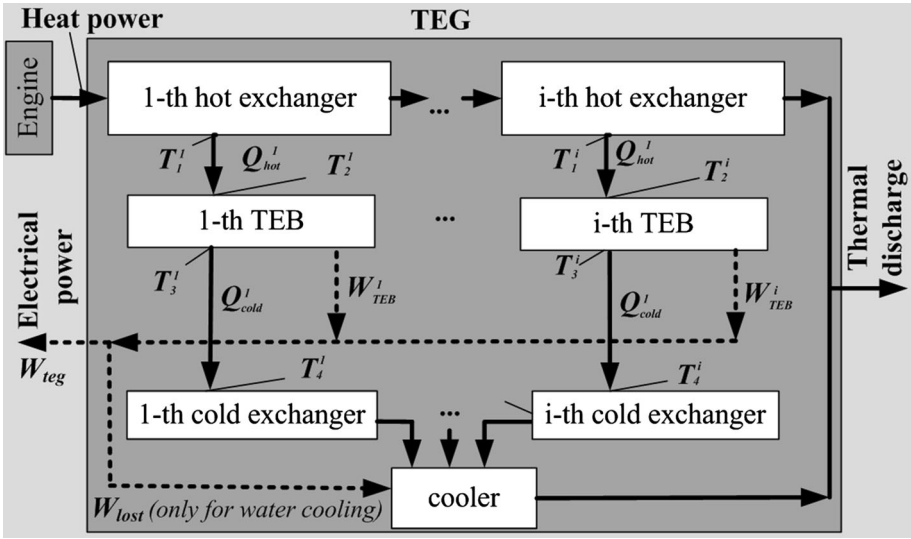

Fig. 2. General schematic of a TEG.

Table I. Boundary conditions used in the CAE model

Design type	Motorcycle	Snowmobile	Water cooled
Ambient temperature (°C)	20	−20	20
Ambient pressure (Pa)		101,325	
Cooling	100 km h^{-1} air velocity	60 km h^{-1} air velocity	α_c = 1070 (W m^{-2} K^{-1})
Exhaust gas flow (kg s^{-1})		0.035	
Exhaust gas temperature (°C)		800	

system, and are equal to the average electrical power consumed by the pumps and fan of the forced hydraulic cooling system ($W_{\mathrm{Lost}} \approx 27$ W).

Heat Transfer Equations for the *i*th Section of the TEG

The thermal flows through the hot and cold heat exchangers are based on Fourier thermal equations in integral form:

$$Q^i_{\mathrm{hot}} = \left[\frac{\delta_{\mathrm{A}}}{0.5(S_1+S_2)\lambda_A} + \frac{\delta_{\mathrm{case}}}{S_2\lambda_{\mathrm{case}}} + R_{\mathrm{hot}}\right]^{-1}(T^i_1 - T^i_2),$$
$$Q^i_{\mathrm{cold}} = \left[\frac{\delta_{\mathrm{C}}}{0.5(S_3+S_4)\lambda_C} + \frac{\delta_{\mathrm{case}}}{S_3\lambda_{\mathrm{case}}} + R_{\mathrm{cold}}\right]^{-1}(T^i_3 - T^i_4), \quad (1)$$

where S_1, S_2, S_3, and S_4 are the average areas of the hot heat exchanger's internal surfaces, hot and cold

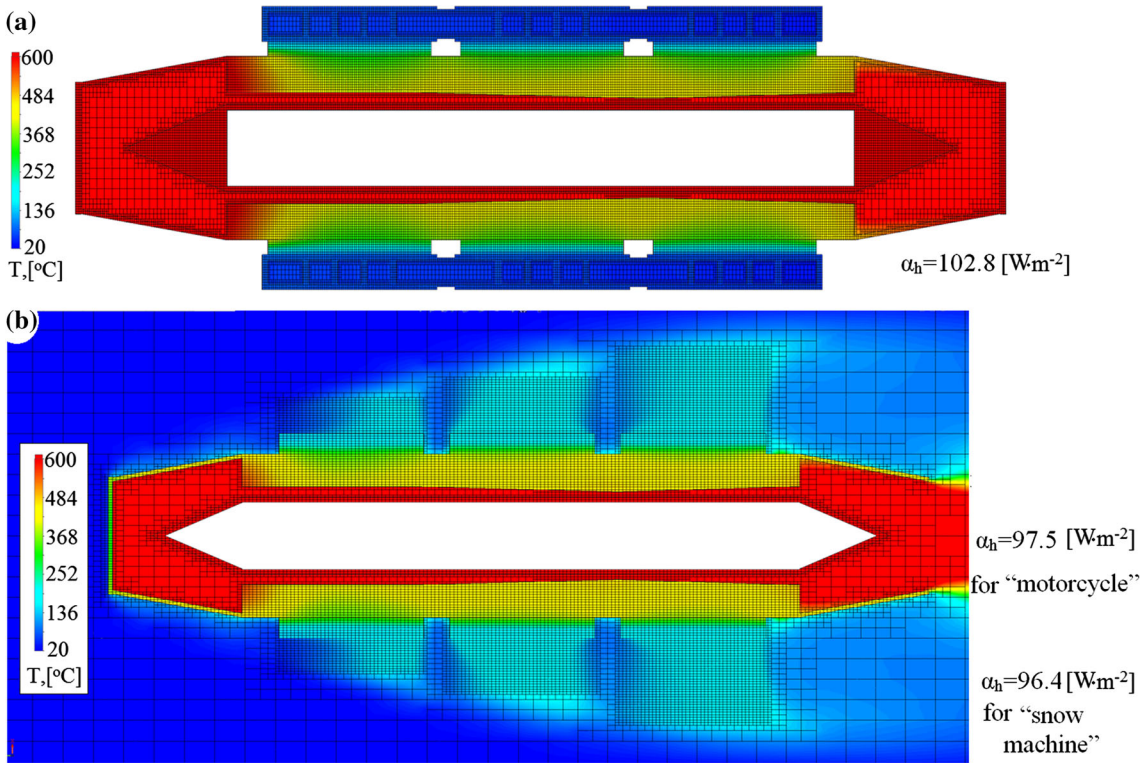

Fig. 3. Results of CAE modeling. Temperature fields (°C) and heat-exchange coefficients of the hot heat exchanger α_h (W m^{-2} K^{-1}) for the two TEG arrangements: (a) water cooled, (b) air cooled.

Table II. Heat-exchange coefficient of the cold α_c heat exchanger as a function of vehicle velocity V_{motion}

V_{motion} (km h^{-1})	α_c (W m^{-2} K^{-1})
10	3.35
20	6.38
40	12.04
60	17.39
80	22.13
100	25.76
120	29.43

thermoelectric battery junctions, and thermoelectric battery (TEB) water cooling loop, respectively; Q^i_{hot} and Q^i_{cold} are the total thermal flows through the ith hot heat exchanger and the ith cold heat exchanger, respectively; δ_{case} and λ_{case} are the average height and thermal conductivity of the TEB wall, respectively; δ_A and λ_A are the average height and thermal conductivity of the hot heat exchanger, respectively; δ_C and λ_C are the average thickness and thermal conductivity of the cold heat exchanger, respectively; and R_{hot} and R_{cold} are the sums of the contact thermal resistance at the hot and cold thermoelectric battery junctions, respectively, which can be determined experimentally[10] or via empirical studies.[11] In this work, the contact thermal resistances R_{hot} and R_{cold} were evaluated experimentally based on a thermal imaging survey of the TEG mock-up ("Appendix"). The thermal resistance of the hot junctions R_{hot} was found to be five times greater than that of the cold junctions R_{cold}. The reason is that the heat sink compound was not used at the hot junctions because of the high temperatures. We show below that the thermal resistance R_{hot} significantly affects the operating characteristics of the TEG.

The thermal conductivity equation for the thermoelectric battery that takes into account the volumetric transfer of thermal power Q^i_{hot} into electrical power W^i_{teb} can be expressed as follows:

$$Q^i_{hot} - \frac{W^i_{teb}}{2} = Q^i_{cold} + \frac{W^i_{teb}}{2} = \left[\frac{\delta_B}{0.5(S_2 + S_3)\bar{\lambda}_B}\right]^{-1}(T^i_2 - T^i_3), \quad (2)$$

where $\bar{\lambda}_B$ and δ_B are the averaged thermal conductivity of the thermoactive material and the height of the thermoelements in the TEB.

For the external surfaces of the hot and cold heat exchangers, the condition of convective heat exchange is assumed, which takes fins into account by means of the finning correction and the flow enhancement coefficients k_{i_eg} and k_{i_w}:

$$Q^i_{\text{hot}} = k_{i\_\text{eg}}\alpha_\text{h}S_1\left(T^i_\text{eg} - T^i_1\right),$$
$$Q^i_{\text{cold}} = k_{i\_w}\alpha_\text{c}S_4\left[T^i_4 - 0.5\left(T^i_{w1} + T^i_{w2}\right)\right], \quad (3)$$

where α_h and α_c are the heat loss coefficients of the hot and cold heat exchangers, respectively; T^i_{w1} and T^i_{w2} are the cooling water temperature of the TEG input and output, respectively; and T^i_eg is the exhaust gas temperature at the ith section input. The total thermal resistance on the hot and cold sides is the sum of the convective heat transfer resistances, the contact thermal resistances at the hot and cold junctions (R_hot and R_cold), and the resistances of the heat exchangers' walls.

Thermoelectric Effects for the ith Section of the TEG

The thermoelectric figure-of-merit for the TEG can be expressed as follows:

$$z = \frac{\bar{\alpha}^2_\text{teg}}{\bar{\rho}_{e\_\text{teg}}\bar{\lambda}_\text{B}\left(1+\varepsilon_\kappa\right)\left(1+\varepsilon_p\right)}, \quad (4)$$

where $\bar{\alpha}_\text{teg}$, $\bar{\rho}_{e\_\text{teg}}$, and $\bar{\lambda}_\text{B}$ are the averaged Seebeck coefficient, resistivity, and heat transfer coefficient of the thermoelectric battery materials, respectively; and ε_p and ε_κ are the coefficients which correct for the electric losses over the switching layers and heat leakages over protective coatings, respectively (for the calculations, the following values were assumed $\varepsilon_p = 6 \times 10^{-2}$, $\varepsilon_\kappa = 5 \times 10^{-2}$).

Accordingly, the efficiency and output electrical power of the ith section of the thermoelectric battery can be expressed as

$$\eta^i_\text{hot} = \frac{\left(T^i_2 - T^i_3\right)}{T^i_2}\frac{M^i - 1}{M^{hi} + \frac{T^i_3}{T^i_2}}, \quad W^i_\text{ted} = \eta^t_\text{teb}Q^i_\text{hot}. \quad (5)$$

where

$$M^i = \sqrt{1 + z0.5\left(T^i_2 - T^i_3\right)}. \quad (6)$$

The geometry of the thermoelements (number of N branch pairs and cross-section areas) of the p-type and n-type branches (S_p and S_n) were determined as follows:

$$N^i = \frac{V_\text{teg}}{2\bar{\alpha}_\text{teg}\left(T^i_2 - T^i_3\right)}\frac{M+1}{M}, \quad (7)$$

$$S_p = \frac{1}{\Theta M}\frac{1}{1+\Psi}\frac{Q^i_\text{hot}\delta_\text{B}}{\bar{\lambda}_\text{B}\left(T^i_2 - T^i_3\right)N^i}\frac{1-\eta_\text{teg}/2}{1+\varepsilon_\kappa}, \quad S_n = \Psi S_p, \quad (8)$$

where

$$\Psi = \sqrt{\frac{\rho_{e\_n}\lambda_p}{\rho_{e\_p}\lambda_n}}, \quad \Theta = 1 + z\frac{0.5\left(T^i_2 + T^i_3\right) + M\cdot T^i_2}{\left(1+M\right)^2}. \quad (9)$$

V_teg is the electrical voltage on the thermoelectric battery, and Θ is the correction factor, which includes thermal conductivity increase from the action of thermoelectric effects.[12]

The required parameters of the thermoelectric battery structure and the electrical power produced by the generator may be determined for the specified thermoelectric materials, the height of the TEB thermoelements, the required voltage V, and the thermal mode.

Parameters Calculation Technique for the ith Section of the TEG

The minimum possible number of variables was selected to determine the unknown variables:

$$Q^i_\text{hot}, T^i_1, T^i_2, T^i_3, T^i_4, T^i_{w2}. \quad (10)$$

The system of six nonlinear algebraic equations for thermal flows (4), (5), (6), and (8) was used as the resolving system. The reasons for nonlinearity are as follows:

- the properties of liquid and gas depend on the temperatures $\rho_\text{eg}(T)$, $\rho_\text{w}(T)$, $\lambda_\text{eg}(T)$, $\lambda_\text{w}(T)$, and $\mu_\text{w}(T)$. These characteristics are defined by the interpolating dependences on the reference data.[13]
- the TEG dependence is nonlinear: $W_\text{teb} = \sum_i W^i_\text{teb}$ = function $(Q^i_\text{hot}, T^i_2, T^i_3)$.

The resolving system was solved in MATLAB by searching for the quadratic error minimum using the Nelder–Mead method.[14]

For the water-cooled TEG, the output power was determined, while considering the power loss on work forced cooling $W_\text{teg} = W_\text{teb} - W_\text{cooling}$.

RESULTS

This section analyzes the impact of the thermoelements' height δ_B and the contact thermal resistance at the hot junctions R_hot on the performance of different types of TEG. The TEG characteristics modeling was carried out for three arrangements at various TEB thicknesses δ_B = 3–25 mm and vehicle velocities. R_hot resistance can be reduced by means of technological solutions.[11] Consequently, we considered the range from the measured value $R_\text{hot} = 9.14 \times 10^{-2}$ K W^{-1} to the limiting value $R_\text{hot} = 0$.

Figure 4 shows the temperature distribution in different TEB sections with different thicknesses for the water cooling arrangement. It is evident from the graph that the section temperatures are very close, as the exhaust cooling is compensated by the increase in the radiator fins. It can be seen that the temperature drop of the hot heat exchanger $T^i_1 - T^i_2$ is significantly greater than that of the cold heat

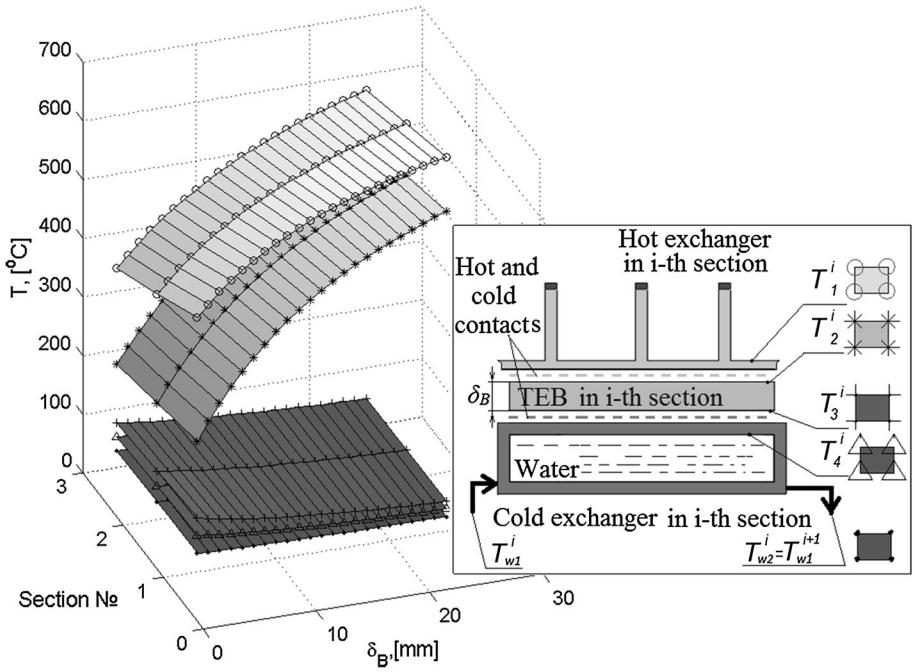

Fig. 4. Temperatures for different sections as a function of the thermoelement's height δ_B for the water-cooled TEG, calculated with contact thermal resistance R_{hot} = 0.0017 m^2 K W^{-1}. T_1^i and T_4^i are the temperatures of the external sides' hot and cold exchangers, respectively; T_2^i and T_3^i are the hot and cold sides of the TEB, respectively; and T_{w2}^i is the water output temperature.

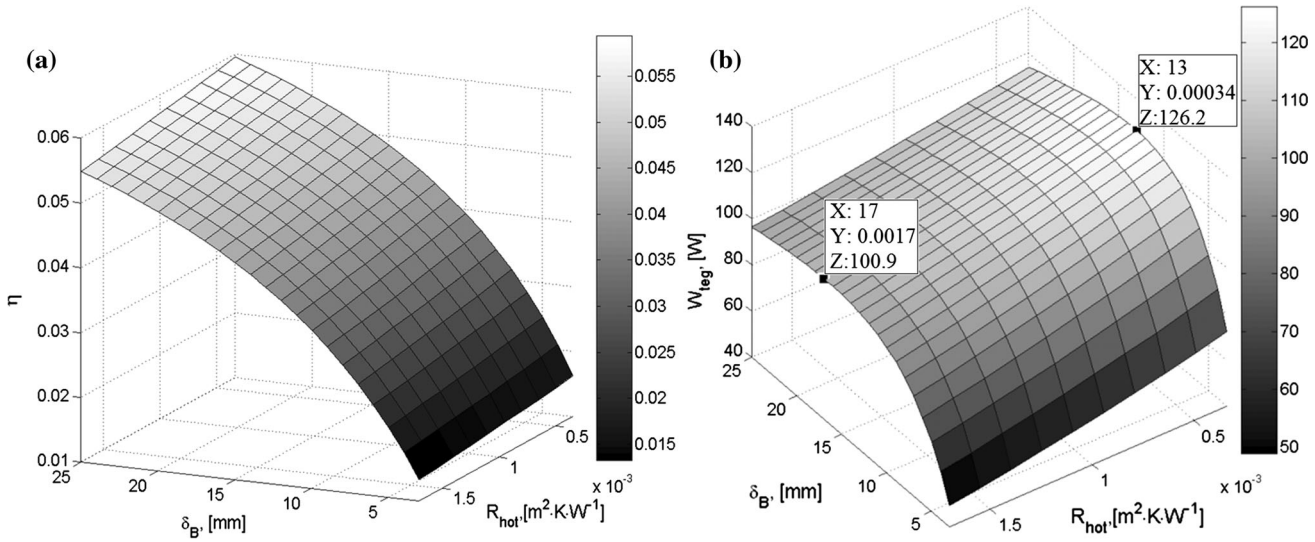

Fig. 5. The thermoelement's thickness δ_B and hot contact thermal resistance R_{hot} determines the TEG characteristics with (a) efficiency η_{teb} and (b) generated electrical power W_{teg}.

exchanger $T_3^i - T_4^i$ owing to the substantial thermal resistance at the hot junctions R_{hot}.

Increasing the TEB height results in an increase in the temperature gradient and an increase in the total thermal resistance. Other types of cooling are characterized by a similar effect according to the height of the temperature distribution.

Figure 5 shows the efficiency η and TEG power W_{teg} as functions of the thermoelectric battery height δ_B and thermal resistance of hot junctions R_{hot}. These data can be useful in selecting the optimum height δ_B for the known thermal resistance R_{hot}, in order to achieve the highest possible TEG generating power. The optimum height of the thermoelements, δ_B, can be reduced from 17 mm to 13 mm when the resistance of the hot layer R_{hot} is decreased. The generator efficiency will constitute 4.5–4.6%, with the generated electrical power varying in the range W_{teg} = 101–126 W. If the contact thermal resistance could be reduced from the

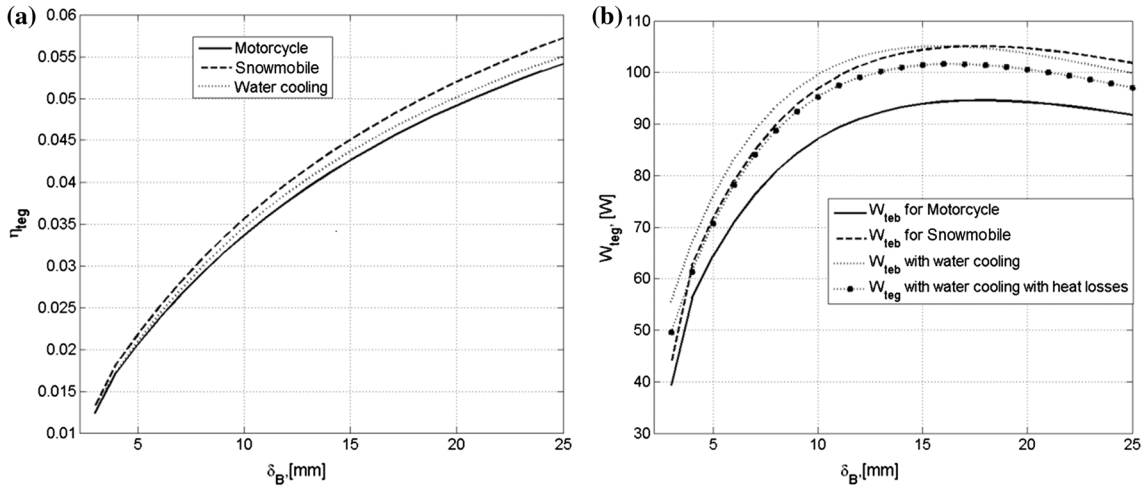

Fig. 6. Influence of thermoelement thickness δ_B on TEG characteristics at R_{hot} = 0.0017 m^2 K W^{-1} V_{moving} = 100 km h^{-1}: (a) efficiency η_{teb}; (b) generated electrical power W_{teg}.

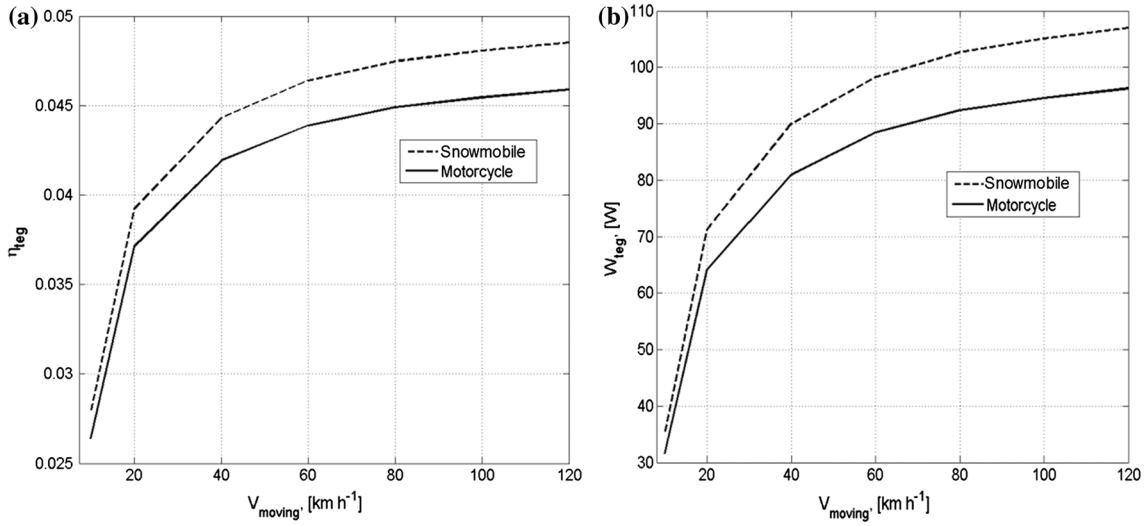

Fig. 7. Influence of vehicle velocity V_{moving} on TEG characteristics at δ_B = 17 mm and R_{hot} = 0.0017 m^2 K W^{-1}: (a) efficiency η_{teb}; (b) generated electrical power W_{teg}.

measured value (R_{hot} = 0.0017 m^2 K W^{-1}) to zero, then the output TEG power would increase by approximately 20%, after which the low value of the heat transfer coefficient α_h for the hot heat exchanger would become the limiting factor.

It may be noted that thermoelectric batteries with relatively high thermoelectric branches are required to achieve a large temperature difference between the hot and cold junctions.

The efficiency η (Fig. 6a) and TEG electrical power W_{teg} (Fig. 6b) are presented below as functions of the thermoelement's thickness δ_B. The power values for different arrangements are close. It was also found that the water-cooled motorcycle-type TEG generates the highest level of electrical power W_{teb}. However, with the energy losses for the forced cooling accounted for, the total power W_{teb} can be comparable to or even lower than that of the snowmobile's TEG (air cooled) at the velocity exceeding 100 km h^{-1}.

It should be noted that the efficiency η_{teg} for the motorcycle and snowmobile in the case of air cooling depends on the velocity (Fig. 7) and significantly decreases for $V_{moving} < 40$ km h^{-1}.

CONCLUSIONS

This paper has proposed a nonlinear mathematical model for TEG performance calculation. The model justifies the TEG arrangements under consideration by additional electrical power generation for small-capacity vehicles, without the need for ICE

redesign. However, their installation requires further research including experimental verification, because the additional mass and aerodynamic loads may negatively affect the vehicle power.

The theoretical values obtained for the TEG power indicate the possibility for small-capacity vehicles to function without electromechanical generators. However, the main challenge to the use of TEGs in small-capacity vehicles is ensuring effective heat dissipation. The effectiveness of air-cooled TEGs significantly decreases as the vehicle decelerates, although significant power can be obtained at high velocities on vehicles with passive air cooling. At the same time, further investigation is imperative with regard to the effect of the cold heat exchanger's finning on the vehicle aerodynamics.

Our calculation results indicate that the thermal contact resistances can have a pronounced influence on TEG operation, as the maximum electrical power decreases by more than 20% after the resistances are considered. The values obtained are approximate estimates because the proposed model does not yet account for the time-dependent power decrease due to corrosion and sooting (for diesel engines) of the hot heat exchanger and contamination of the external heat exchanger.

ACKNOWLEDGEMENT

The research work was supported by the Ministry of Education and Science of the Russian Federation (Unique Identifier: RFMEFI57714X0113).

APPENDIX

Table III shows the essential parameters of the Yamaha WR450F IC engine used for calculation.

Table III. Yamaha WR450F internal combustion (IC) engine parameters and operational modes

Exhaust temperatures at TEG input	T^E_{eg1}	1073 K
Rotational speed	n_E	9000 rev min^{-1}
Total engine cylinders volume	$V_{\Sigma cyl}$	0.449
Engine efficiency	η_{Eg}	0.400
IC engine generator efficiency	η_{gen}	0.550
Pump efficiency of the cooling water system	η_{w2}	0.800
TEG parameters		
Average thickness of hot heat exchanger	δ_A	0.003 m
Average thickness of TEB case	δ_{case}	0.0005 m
Average thickness of cold water exchanger	δ_C	0.011 m
Average thickness of TEB wall	δ_D	0.003–0.025 m
Internal part surface area of hot exchanger without fins	S_1	0.0181 m^2
Hot junctures area of TEB	S_2	0.0125 m^2
Cold junctures area of TEB	S_3	0.0125 m^2
Surface of water cold exchanger	S_4	0.0125 m^2
Coolant consumption	G_w	0.15 l s^{-1}
Finning coefficient in flow channel of TEG	k_{i_eg}	2.59
Intensification coefficient of cooling loop flow		
For 1 section motorcycle TEG and snowmobile TEG	k_{1_w}	12
For 2 section motorcycle TEG and snowmobile TEG	k_{2_w}	27
For 3 section motorcycle TEG and snowmobile TEG	k_{3_w}	46
For TEG with water cooling	k_w	2.19
Sums of contact thermal resistance at the hot and cold junctions	R_{hot}	9.14×10^{-2} K W^{-1}
(Experimentally estimated values)	R_{cold}	1.74×10^{-2} K W^{-1}

Table IV. Properties of thermoelectric materials

Material	Type of conductivity	Operating temperature range (°C)	Seebeck coefficient α (V/K)	Resistivity ρ (Ω cm)	Coefficient of thermal conductivity κ, W/(m K)
PbTe	n	200–500	187.1×10^{-6}	30.91×10^{-4}	1.4
GeTe	p	200–500	225.4×10^{-6}	21.37×10^{-4}	1.5

Table IV shows the thermoelectric materials properties used in the calculation.

REFERENCES

1. T. Kajikawa, *J. Thermoelectr.* 1, 19 (2009).
2. L. Weiling and T. Shantung, *Chin. Sci. Bull.* (2004). doi: 10.1360/04we0037.
3. K.T. Wojciechowski, M. Schmidt, R. Zybala, J. Merkisz, P. Fuc, and P. Lijewski, *J. Electron. Mater.* (2010). doi: 10.1007/s11664-009-1010-1.
4. D. Tatarinov, Charakterisierung und Simulation einer thermoelektrischen Generatoranlage zur Energie-Rekuperation aus Abgasen im Pkw (Gradeseines Doktors der Ingenieurwissenschaften Diss. Dr.-Ing, 2015), https://duepublico.uni-duisburg-essen.de/servlets/DerivateServlet/Derivate-40538/Tatarinov_Diss.pdf. Accessed 04 April 2017.
5. M. Jaegle, Multiphysics simulation of thermoelectric systems (Comsol Conference in Hannover, 2008) http://cn.comsol.com/paper/download/37152/Jaegle_pres.pdf. Accessed 23 May 2016.
6. V. Longinotti, S. Di Marco, S. Pistilli, F. Costa, M. Giusti, G. Gammariello, I. Gison, G. Latessa, D. Mascolo, and A. Buosciolo, COMSOL multiphysics simulation integrated into genetic optimization (Comsol Conference in Rotterdam, 2013) http://cn.comsol.com/paper/comsol-multiphysics-simulation-integrated-into-genetic-optimization-16018. Accessed 23 May 2016.
7. A.P. Freedman, A thermoelectric generation subsystem model for heat recovery simulations (M.S. Thesis, Rochester Institute of Technology, 2011) http://scholarworks.rit.edu/cgi/viewcontent.cgi?article=8401&context=theses. Accessed 04 April 2016.
8. R.A. Poshekhonov, A.S. Osipkov, and M.O. Makeev, *GJPAM* 12, 667 (2016).
9. O.V. Marchenko, *Metodi rascheta termoelektricheskikh generatorov (Methods of calculating for thermoelectric generators)* (Novosibirsk: Nauka. Sibirskaja izdatel'skaja firma RAN, 1995), p. 199.
10. Y. Manasian, *Sudovye termojelektricheskie ustrojstva i ustanovki (Ship thermoelectric device and equipment)* (Leningrad: Shipbuilding, 1968), p. 95.
11. A. Bejan and A.D. Kraus, *Heat transfer handbook* (New Jersey, NY: Wiley, 2003), p. 1480.
12. R.V. Kovalskii, *Inzhenernye metody rascheta termojelektricheskih generatorov (Engineering methods for calculation thermoelectric generators)* (Moscow: Nauka, 1990), p. 40.
13. N.B. Vargaftic, *Spravichnic po teplophisicheckim svoistvam gazov a jidkostei (Handbook of thermalphysic properties gases and fluids)* (Moscow: Nauka, 1972).
14. J.C. Lagarias, J.A. Reeds, M.H. Wright, and P.E. Wright, *SIAM J. Optim.* 9, 112 (1998).